FERMILAB-PUB-14-015-E

Evidence for s-channel Single-Top-Quark Production in Events with one Charged Lepton and two Jets at CDF

T. Aaltonen,[21] S. Amerio[jj],[39] D. Amidei,[31] A. Anastassov[v],[15] A. Annovi,[17] J. Antos,[12] G. Apollinari,[15] J.A. Appel,[15] T. Arisawa,[52] A. Artikov,[13] J. Asaadi,[47] W. Ashmanskas,[15] B. Auerbach,[2] A. Aurisano,[47] F. Azfar,[38] W. Badgett,[15] T. Bae,[25] A. Barbaro-Galtieri,[26] V.E. Barnes,[43] B.A. Barnett,[23] P. Barria[ll],[41] P. Bartos,[12] M. Bauce[jj],[39] F. Bedeschi,[41] S. Behari,[15] G. Bellettini[kk],[41] J. Bellinger,[54] D. Benjamin,[14] A. Beretvas,[15] A. Bhatti,[45] K.R. Bland,[5] B. Blumenfeld,[23] A. Bocci,[14] A. Bodek,[44] D. Bortoletto,[43] J. Boudreau,[42] A. Boveia,[11] L. Brigliadori[ii],[6] C. Bromberg,[32] E. Brucken,[21] J. Budagov,[13] H.S. Budd,[44] K. Burkett,[15] G. Busetto[jj],[39] P. Bussey,[19] P. Butti[kk],[41] A. Buzatu,[19] A. Calamba,[10] S. Camarda,[4] M. Campanelli,[28] F. Canelli[cc],[11] B. Carls,[22] D. Carlsmith,[54] R. Carosi,[41] S. Carrillo[l],[16] B. Casal[j],[9] M. Casarsa,[48] A. Castro[ii],[6] P. Catastini,[20] D. Cauz[qqrr],[48] V. Cavaliere,[22] M. Cavalli-Sforza,[4] A. Cerri[e],[26] L. Cerrito[q],[28] Y.C. Chen,[1] M. Chertok,[7] G. Chiarelli,[41] G. Chlachidze,[15] K. Cho,[25] D. Chokheli,[13] A. Clark,[18] C. Clarke,[53] M.E. Convery,[15] J. Conway,[7] M. Corbo[y],[15] M. Cordelli,[17] C.A. Cox,[7] D.J. Cox,[7] M. Cremonesi,[41] D. Cruz,[47] J. Cuevas[x],[9] R. Culbertson,[15] N. d'Ascenzo[u],[15] M. Datta[ff],[15] P. de Barbaro,[44] L. Demortier,[45] M. Deninno,[6] M. D'Errico[jj],[39] F. Devoto,[21] A. Di Canto[kk],[41] B. Di Ruzza[p],[15] J.R. Dittmann,[5] S. Donati[kk],[41] M. D'Onofrio,[27] M. Dorigo[ss],[48] A. Driutti[qqrr],[48] K. Ebina,[52] R. Edgar,[31] A. Elagin,[47] R. Erbacher,[7] S. Errede,[22] B. Esham,[22] S. Farrington,[38] J.P. Fernández Ramos,[29] R. Field,[16] G. Flanagan[s],[15] R. Forrest,[7] M. Franklin,[20] J.C. Freeman,[15] H. Frisch,[11] Y. Funakoshi,[52] C. Galloni[kk],[41] A.F. Garfinkel,[43] P. Garosi[ll],[41] H. Gerberich,[22] E. Gerchtein,[15] S. Giagu,[46] V. Giakoumopoulou,[3] K. Gibson,[42] C.M. Ginsburg,[15] N. Giokaris,[3] P. Giromini,[17] G. Giurgiu,[23] V. Glagolev,[13] D. Glenzinski,[15] M. Gold,[34] D. Goldin,[47] A. Golossanov,[15] G. Gomez,[9] G. Gomez-Ceballos,[30] M. Goncharov,[30] O. González López,[29] I. Gorelov,[34] A.T. Goshaw,[14] K. Goulianos,[45] E. Gramellini,[6] S. Grinstein,[4] C. Grosso-Pilcher,[11] R.C. Group,[51, 15] J. Guimaraes da Costa,[20] S.R. Hahn,[15] J.Y. Han,[44] F. Happacher,[17] K. Hara,[49] M. Hare,[50] R.F. Harr,[53] T. Harrington-Taber[m],[15] K. Hatakeyama,[5] C. Hays,[38] J. Heinrich,[40] M. Herndon,[54] A. Hocker,[15] Z. Hong,[47] W. Hopkins[f],[15] S. Hou,[1] R.E. Hughes,[35] U. Husemann,[55] M. Hussein[aa],[32] J. Huston,[32] G. Introzzi[nnoo],[41] M. Iori[pp],[46] A. Ivanov[o],[7] E. James,[15] D. Jang,[10] B. Jayatilaka,[15] E.J. Jeon,[25] S. Jindariani,[15] M. Jones,[43] K.K. Joo,[25] S.Y. Jun,[10] T.R. Junk,[15] M. Kambeitz,[24] T. Kamon,[25, 47] P.E. Karchin,[53] A. Kasmi,[5] Y. Kato[n],[37] W. Ketchum[gg],[11] J. Keung,[40] B. Kilminster[cc],[15] D.H. Kim,[25] H.S. Kim,[25] J.E. Kim,[25] M.J. Kim,[17] S.H. Kim,[49] S.B. Kim,[25] Y.J. Kim,[25] Y.K. Kim,[11] N. Kimura,[52] M. Kirby,[15] K. Knoepfel,[15] K. Kondo,[52, *] D.J. Kong,[25] J. Konigsberg,[16] A.V. Kotwal,[14] M. Kreps,[24] J. Kroll,[40] M. Kruse,[14] T. Kuhr,[24] M. Kurata,[49] A.T. Laasanen,[43] S. Lammel,[15] M. Lancaster,[28] K. Lannon[w],[35] G. Latino[ll],[41] H.S. Lee,[25] J.S. Lee,[25] S. Leo,[41] S. Leone,[41] J.D. Lewis,[15] A. Limosani[r],[14] E. Lipeles,[40] A. Lister[a],[18] H. Liu,[51] Q. Liu,[43] T. Liu,[15] S. Lockwitz,[55] A. Loginov,[55] D. Lucchesi[jj],[39] A. Lucà,[17] J. Lueck,[24] P. Lujan,[26] P. Lukens,[15] G. Lungu,[45] J. Lys,[26] R. Lysak[d],[12] R. Madrak,[15] P. Maestro[ll],[41] S. Malik,[45] G. Manca[b],[27] A. Manousakis-Katsikakis,[3] L. Marchese[hh],[6] F. Margaroli,[46] P. Marino[mm],[41] M. Martínez,[4] K. Matera,[22] M.E. Mattson,[53] A. Mazzacane,[15] P. Mazzanti,[6] R. McNulty[i],[27] A. Mehta,[27] P. Mehtala,[21] C. Mesropian,[45] T. Miao,[15] D. Mietlicki,[31] A. Mitra,[1] H. Miyake,[49] S. Moed,[15] N. Moggi,[6] C.S. Moon[y],[15] R. Moore[ddee],[15] M.J. Morello[mm],[41] A. Mukherjee,[15] Th. Muller,[24] P. Murat,[15] M. Mussini[ii],[6] J. Nachtman[m],[15] Y. Nagai,[49] J. Naganoma,[52] I. Nakano,[36] A. Napier,[50] J. Nett,[47] C. Neu,[51] T. Nigmanov,[42] L. Nodulman,[2] S.Y. Noh,[25] O. Norniella,[22] L. Oakes,[38] S.H. Oh,[14] Y.D. Oh,[25] I. Oksuzian,[51] T. Okusawa,[37] R. Orava,[21] L. Ortolan,[4] C. Pagliarone,[48] E. Palencia[e],[9] P. Palni,[34] V. Papadimitriou,[15] W. Parker,[54] G. Pauletta[qqrr],[48] M. Paulini,[10] C. Paus,[30] T.J. Phillips,[14] G. Piacentino,[41] E. Pianori,[40] J. Pilot,[7] K. Pitts,[22] C. Plager,[8] L. Pondrom,[54] S. Poprocki[f],[15] K. Potamianos,[26] A. Pranko,[26] F. Prokoshin[z],[13] F. Ptohos[g],[17] G. Punzi[kk],[41] N. Ranjan,[43] I. Redondo Fernández,[29] P. Renton,[38] M. Rescigno,[46] F. Rimondi,[6, *] L. Ristori,[41, 15] A. Robson,[19] T. Rodriguez,[40] S. Rolli[h],[50] M. Ronzani[kk],[41] R. Roser,[15] J.L. Rosner,[11] F. Ruffini[ll],[41] A. Ruiz,[9] J. Russ,[10] V. Rusu,[15] W.K. Sakumoto,[44] Y. Sakurai,[52] L. Santi[qqrr],[48] K. Sato,[49] V. Saveliev[u],[15] A. Savoy-Navarro[y],[15] P. Schlabach,[15] E.E. Schmidt,[15] T. Schwarz,[31] L. Scodellaro,[9] F. Scuri,[41] S. Seidel,[34] Y. Seiya,[37] A. Semenov,[13] F. Sforza[kk],[41] S.Z. Shalhout,[7] T. Shears,[27] P.F. Shepard,[42] M. Shimojima[t],[49] M. Shochet,[11] I. Shreyber-Tecker,[33] A. Simonenko,[13] K. Sliwa,[50] J.R. Smith,[7] F.D. Snider,[15] H. Song,[42] V. Sorin,[4] R. St. Denis,[19] M. Stancari,[15] D. Stentz[v],[15] J. Strologas,[34] Y. Sudo,[49] A. Sukhanov,[15] I. Suslov,[13] K. Takemasa,[49] Y. Takeuchi,[49] J. Tang,[11] M. Tecchio,[31] P.K. Teng,[1] J. Thom[f],[15] E. Thomson,[40] V. Thukral,[47] D. Toback,[47] S. Tokar,[12] K. Tollefson,[32] T. Tomura,[49] D. Tonelli[e],[15] S. Torre,[17] D. Torretta,[15] P. Totaro,[39]

Operated by Fermi Research Alliance, LLC under Contract No. De-AC02-07CH11359 with the United States Department of Energy.

M. Trovato[mm],[41] F. Ukegawa,[49] S. Uozumi,[25] F. Vázquez[l],[16] G. Velev,[15] C. Vellidis,[15] C. Vernieri[mm],[41] M. Vidal,[43] R. Vilar,[9] J. Vizán[bb],[9] M. Vogel,[34] G. Volpi,[17] P. Wagner,[40] R. Wallny[j],[15] S.M. Wang,[1] D. Waters,[28] W.C. Wester III,[15] D. Whiteson[c],[40] A.B. Wicklund,[2] S. Wilbur,[7] H.H. Williams,[40] J.S. Wilson,[31] P. Wilson,[15] B.L. Winer,[35] P. Wittich[f],[15] S. Wolbers,[15] H. Wolfe,[35] T. Wright,[31] X. Wu,[18] Z. Wu,[5] K. Yamamoto,[37] D. Yamato,[37] T. Yang,[15] U.K. Yang,[25] Y.C. Yang,[25] W.-M. Yao,[26] G.P. Yeh,[15] K. Yi[m],[15] J. Yoh,[15] K. Yorita,[52] T. Yoshida[k],[37] G.B. Yu,[14] I. Yu,[25] A.M. Zanetti,[48] Y. Zeng,[14] C. Zhou,[14] and S. Zucchelli[ii]6

(CDF Collaboration)[†]

[1] *Institute of Physics, Academia Sinica, Taipei, Taiwan 11529, Republic of China*
[2] *Argonne National Laboratory, Argonne, Illinois 60439, USA*
[3] *University of Athens, 157 71 Athens, Greece*
[4] *Institut de Fisica d'Altes Energies, ICREA, Universitat Autonoma de Barcelona, E-08193, Bellaterra (Barcelona), Spain*
[5] *Baylor University, Waco, Texas 76798, USA*
[6] *Istituto Nazionale di Fisica Nucleare Bologna, [ii] University of Bologna, I-40127 Bologna, Italy*
[7] *University of California, Davis, Davis, California 95616, USA*
[8] *University of California, Los Angeles, Los Angeles, California 90024, USA*
[9] *Instituto de Fisica de Cantabria, CSIC-University of Cantabria, 39005 Santander, Spain*
[10] *Carnegie Mellon University, Pittsburgh, Pennsylvania 15213, USA*
[11] *Enrico Fermi Institute, University of Chicago, Chicago, Illinois 60637, USA*
[12] *Comenius University, 842 48 Bratislava, Slovakia; Institute of Experimental Physics, 040 01 Kosice, Slovakia*
[13] *Joint Institute for Nuclear Research, RU-141980 Dubna, Russia*
[14] *Duke University, Durham, North Carolina 27708, USA*
[15] *Fermi National Accelerator Laboratory, Batavia, Illinois 60510, USA*
[16] *University of Florida, Gainesville, Florida 32611, USA*
[17] *Laboratori Nazionali di Frascati, Istituto Nazionale di Fisica Nucleare, I-00044 Frascati, Italy*
[18] *University of Geneva, CH-1211 Geneva 4, Switzerland*
[19] *Glasgow University, Glasgow G12 8QQ, United Kingdom*
[20] *Harvard University, Cambridge, Massachusetts 02138, USA*
[21] *Division of High Energy Physics, Department of Physics, University of Helsinki, FIN-00014, Helsinki, Finland; Helsinki Institute of Physics, FIN-00014, Helsinki, Finland*
[22] *University of Illinois, Urbana, Illinois 61801, USA*
[23] *The Johns Hopkins University, Baltimore, Maryland 21218, USA*
[24] *Institut für Experimentelle Kernphysik, Karlsruhe Institute of Technology, D-76131 Karlsruhe, Germany*
[25] *Center for High Energy Physics: Kyungpook National University, Daegu 702-701, Korea; Seoul National University, Seoul 151-742, Korea; Sungkyunkwan University, Suwon 440-746, Korea; Korea Institute of Science and Technology Information, Daejeon 305-806, Korea; Chonnam National University, Gwangju 500-757, Korea; Chonbuk National University, Jeonju 561-756, Korea; Ewha Womans University, Seoul, 120-750, Korea*
[26] *Ernest Orlando Lawrence Berkeley National Laboratory, Berkeley, California 94720, USA*
[27] *University of Liverpool, Liverpool L69 7ZE, United Kingdom*
[28] *University College London, London WC1E 6BT, United Kingdom*
[29] *Centro de Investigaciones Energeticas Medioambientales y Tecnologicas, E-28040 Madrid, Spain*
[30] *Massachusetts Institute of Technology, Cambridge, Massachusetts 02139, USA*
[31] *University of Michigan, Ann Arbor, Michigan 48109, USA*
[32] *Michigan State University, East Lansing, Michigan 48824, USA*
[33] *Institution for Theoretical and Experimental Physics, ITEP, Moscow 117259, Russia*
[34] *University of New Mexico, Albuquerque, New Mexico 87131, USA*
[35] *The Ohio State University, Columbus, Ohio 43210, USA*
[36] *Okayama University, Okayama 700-8530, Japan*
[37] *Osaka City University, Osaka 558-8585, Japan*
[38] *University of Oxford, Oxford OX1 3RH, United Kingdom*
[39] *Istituto Nazionale di Fisica Nucleare, Sezione di Padova, [jj] University of Padova, I-35131 Padova, Italy*
[40] *University of Pennsylvania, Philadelphia, Pennsylvania 19104, USA*
[41] *Istituto Nazionale di Fisica Nucleare Pisa, [kk] University of Pisa, [ll] University of Siena, [mm] Scuola Normale Superiore, I-56127 Pisa, Italy, [nn] INFN Pavia, I-27100 Pavia, Italy, [oo] University of Pavia, I-27100 Pavia, Italy*
[42] *University of Pittsburgh, Pittsburgh, Pennsylvania 15260, USA*
[43] *Purdue University, West Lafayette, Indiana 47907, USA*
[44] *University of Rochester, Rochester, New York 14627, USA*
[45] *The Rockefeller University, New York, New York 10065, USA*

[46] Istituto Nazionale di Fisica Nucleare, Sezione di Roma 1,
[pp] Sapienza Università di Roma, I-00185 Roma, Italy
[47] Mitchell Institute for Fundamental Physics and Astronomy,
Texas A&M University, College Station, Texas 77843, USA
[48] Istituto Nazionale di Fisica Nucleare Trieste, [qq] Gruppo Collegato di Udine,
[rr] University of Udine, I-33100 Udine, Italy, [ss] University of Trieste, I-34127 Trieste, Italy
[49] University of Tsukuba, Tsukuba, Ibaraki 305, Japan
[50] Tufts University, Medford, Massachusetts 02155, USA
[51] University of Virginia, Charlottesville, Virginia 22906, USA
[52] Waseda University, Tokyo 169, Japan
[53] Wayne State University, Detroit, Michigan 48201, USA
[54] University of Wisconsin, Madison, Wisconsin 53706, USA
[55] Yale University, New Haven, Connecticut 06520, USA

(Dated: January 28, 2014)

We report evidence for s-channel single-top-quark production in proton-antiproton collisions at center-of-mass energy $\sqrt{s} = 1.96$ TeV using a data set that corresponds to an integrated luminosity of 9.4 fb^{-1} collected by the Collider Detector at Fermilab. We select events consistent with the s-channel process including two jets and one leptonically decaying W boson. The observed significance is 3.8 standard deviations with respect to the background-only prediction. Assuming a top-quark mass of 172.5 GeV/c^2, we measure the s-channel cross section to be $1.41^{+0.44}_{-0.42}$ pb.

In proton-antiproton collisions, top quarks can be produced singly through electroweak interactions. This process provides a unique opportunity to test the standard model (SM) and search for non-SM physics. Each channel of the single-top-quark process is sensitive to different classes of SM extensions: the s-channel process, in which an intermediate W boson decays into a top (antitop) quark and an antibottom (bottom) quark, is sensitive to contributions from additional heavy bosons [1]; the t-channel process, in which a bottom quark transforms into a top quark by exchanging a W boson with another quark, is more sensitive to flavor-changing neutral currents [1]. Independently studying the production rate of these channels provides more restrictive constraints on SM extensions than just studying the combined production rate [2].

Single-top-quark production was first observed independently by the CDF and D0 experiments in 2009 [3, 4]. The t-channel production was first observed in 2011 by the D0 experiment [5], and confirmed in 2012 by the ATLAS [6] and CMS [7] experiments. The ATLAS [8] and CMS [9] experiments also reported evidence for top-quark associated production with a W boson. The s-channel process has not yet been observed. Because of the smaller production cross section and larger backgrounds, it is more difficult to isolate it compared to the t-channel process in proton-antiproton collisions. It is even more difficult at the LHC, as proton-proton collisions yield a significantly smaller signal-to-background ratio compared to the Tevatron. Recently the D0 collaboration announced the first evidence for the s-channel process in the ℓ+jets channel with a data set corresponding to 9.7 fb^{-1} of integrated luminosity [10].

In this Letter, we present the measurement of the single-top-quark s-channel cross section with the full CDF Run II data set in the ℓ+jets final state. The data are collected with the general-purpose Collider Detector at Fermilab (CDF II) [11] and correspond to an integrated luminosity of 9.4 fb^{-1}. The CDF II detector is a solenoid magnetic spectrometer surrounded by calorimeters and muon detectors.

Since top-bottom quark coupling is much larger than the magnitudes of the top-down and top-strange quark couplings, we assume that all top quarks decay into Wb pairs. We select events in which the W boson decays leptonically into an electron or a muon with a corresponding neutrino. Electrons or muons from τ decay are also accepted. Thus, the final state of the signal process consists of one reconstructed electron or muon, one corresponding neutrino, and two jets originating from bottom quarks (b jets). Since the final state of this process is the same one as used in the search for a Higgs boson (H) produced in association with a W boson [12], the techniques used in this Letter are based on this recent search but with a discriminant optimized for the present measurement.

There are important differences in the jet selection strategy between this s-channel-optimized analysis and the previous measurements [13], which were optimized for the t-channel process. The t-channel process usually yields one light-flavor jet in the forward region (pseudorapidity $|\eta| > 2.0$), which is crucial to distinguish the t-channel signal from background events. Since including these forward jets does not lead to a more powerful discriminator for the s-channel measurement, only central jets ($|\eta| < 2.0$) are included. Moreover, for the s-channel process, events with two b jets provide the most sensitivity, while most t-channel events have only one reconstructable b jet. As a result, the sensitivity of the s-channel analysis is improved with a more efficient b-jet selection algorithm [14].

Events are collected using three classes of online selection requirements (triggers). In order to improve the lep-

ton acceptance, a novel inclusive trigger strategy is used for events including a central electron or central muon ($|\eta| < 1.0$) with large transverse momentum p_T [15]. This improves the trigger efficiency by 4.7% for electrons and 12.6% for muons compared to the previous single-top-quark cross section measurement [3]. The details of this technique are discussed in Ref. [12]. Events triggered by $\not\!\!E_T$-based triggers [15], which require $\not\!\!E_T > 45$ GeV or $\not\!\!E_T > 35$ GeV plus two jets, are also included. These events allow the inclusion of additional identified muon types and are referred to as the extended muon category [13].

The algorithms for identifying leptons and jets are the same as those used in Ref. [13]. Events passing the trigger requirements are further selected by requiring exactly one isolated charged lepton with reconstructed transverse momentum $p_T > 20$ GeV/c. The $\not\!\!E_T$ threshold is 20 GeV for events containing central electrons and extended muons, and 10 GeV for events containing central muons. Events are also required to have exactly two jets with transverse energy $E_T > 20$ GeV and pseudorapidity $|\eta| < 2.0$. A support-vector-machine algorithm [16] is used to reduce the contamination from multijet events that do not contain a W boson.

The invariant mass of the reconstructed top-quark candidate provides the greatest discrimination between s-channel single-top-quark events and non-top-quark backgrounds. The z-component of the neutrino momentum is necessary for the invariant-mass calculation and can be quadratically constrained by implementing the W-boson invariant-mass requirement. We choose the smaller solution when there are two real solutions for this variable. Correctly selecting the b jet that originated from top-quark decay is necessary to improve the mass resolution of the reconstructed top quark. A neural network is employed to select the right jet out of the two candidate jets in each event. The neural network uses the following information on both jets: jet transverse momentum, p_T; invariant mass of the lepton and one jet, $M_{\ell j}$; invariant mass of the lepton, the neutrino and one jet, $M_{\ell\nu j}$; and the jet direction in the off-shell W-boson rest frame, $\cos\theta_j$. This algorithm selects the correct jet in 84% of simulated SM single-top-quark s-channel events.

To further suppress backgrounds, such as light-flavor jets produced in association with a W boson, at least one of the two jets in each event is required to be a b jet. Because there are several observable properties of b jets that can be used to discriminate them from other jets, a neural-network tagging algorithm [14] is used to preferentially select b jets. Jets are classified based on the output value of the algorithm as untagged, loose (L), or tight (T) tagged. For T (L) jets, as measured from simulation, the efficiency for selecting true b jets is 42%$\pm$1.6% (70%$\pm$6.5%), while the misidentification rate for charm-quark jets is 8.5%$\pm$0.7% (27%$\pm$5%), and the misidentification rate for jets originating from other quarks and gluons is 0.89%$\pm$0.16% (8.9%$\pm$0.9%). By applying these tagging requirements to each jet in an event, we construct four non-overlapping tagging categories: TT, TL, T, and LL. For the double-tag categories, the category with the highest signal-to-background ratio is chosen if an event satisfies more than one category; for the single-tag category, one jet of the event is required to be tight tagged and the other one is untagged.

Signal and background events are modeled using a combination of data-driven methods and Monte Carlo (MC) simulation including the CDF II detector response modeled by GEANT3 [17]. The single-top-quark events are modeled using POWHEG [18] with the top-quark mass set to 172.5 GeV/c^2, while quark shower and hadronization are performed by PYTHIA [19]. Signal events generated by POWHEG are at next-to-leading-order (NLO) accuracy in the strong coupling α_s, which is an improved model compared to the leading-order model used in Ref. [13]. The background model remains unchanged from the previous measurement [13]. The diboson (WW, WZ, ZZ), $t\bar{t}$, and Higgs-boson processes (with the Higgs-boson mass set to 125 GeV/c^2) are modeled using simulated events generated with PYTHIA and normalized to the cross section calculated in Refs. [20–22]. Events in which a W or Z boson is produced in association with jets (W/Z+jets) are generated with ALPGEN [23] at leading order and their hadronic shower simulated with PYTHIA. The background from the multijet process, which does not contain a W boson, is predicted using a data-driven model. The normalizations of multijet and W+jets processes are determined in a control sample (pretag sample) that includes events without any b-tag requirement. There are 122 039 events in the pretag sample, which is dominated by W+jets and multijet events. Since multijet events typically have smaller $\not\!\!E_T$ than W-boson events, their normalizations are determined by fitting the $\not\!\!E_T$ distribution in the control sample. Normalization in the b-tagged signal sample for the W+heavy-flavor-jets background is calculated by applying the tagging efficiency and the fraction of heavy-flavor jets to the rates calculated in the pretag sample. For the W+light-flavor background, where one or two jets are misidentified as a b jet, the normalization is calculated from the W+jets pretag sample by subtracting the heavy-flavor fraction and multiplying by the per-jet b-tag misidentification rate. For the multijet background, a b-tag rate derived from data is used to estimate the normalization of the tagged multijet background.

The estimated event yields are shown in Table I. Here, and in all following figures, we combine b-tag categories with similar signal purity (TT with TL and T with LL). Table I shows that the predicted background and its uncertainty are larger than the expected signal. By using variables with different distributions for signal and backgrounds, we improve signal purity in some regions of these distributions. The invariant mass distribution of

top-quark candidates, shown in Fig. 1, is the most powerful single discriminating variable.

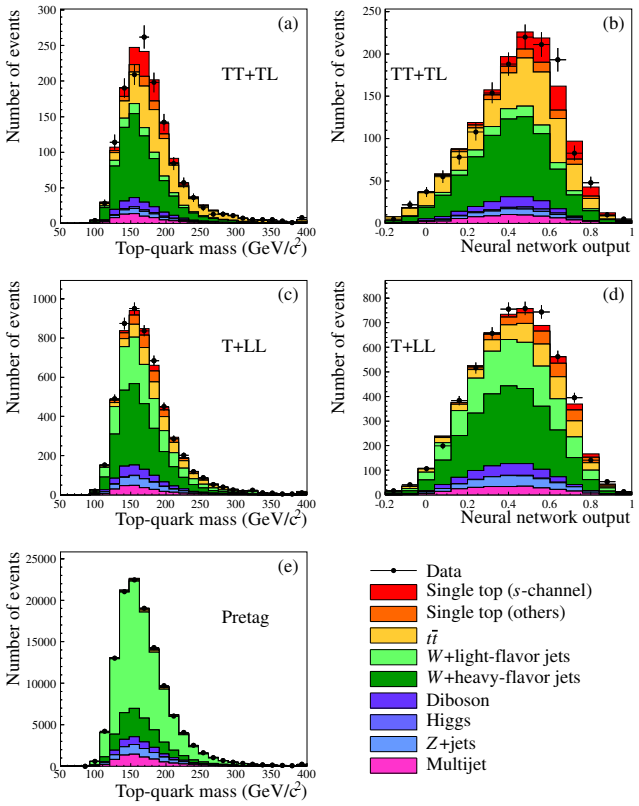

FIG. 1. Distribution of invariant mass of the reconstructed top-quark candidates (left), and distribution of the neural network output (right). We combine b-tag categories with comparable signal purity: TT+TL for panels (a) and (b), and T+LL for panels (c) and (d). Events in the pretag control sample are shown in panel (e). Statistical uncertainties are shown for the data points.

We train a set of artificial neural networks [24] to further discriminate the signal process using the combined information on the reconstructed top-quark mass and several other variables. The neural networks incorporate the following variables: invariant mass of the top-quark candidate, $M_{\ell\nu j}$; invariant mass of all signal final-state particles, $M_{\ell\nu jj}$; transverse momentum of the charged lepton, p_T^{ℓ}; invariant mass of the two jets, M_{jj}; angle between the charged-lepton momentum and the momentum of the jet from the top-quark decay in the top-quark rest frame, $\cos\theta_{\ell j}$; scalar sum of transverse energy of the two jets, the charged lepton, and the neutrino, H_T; transverse mass of the top-quark candidate, $M_T^{\ell\nu j}$, defined to be the invariant mass calculated using the projections of the three-momentum components in the plane perpendicular to the beam axis; and output value of the neural network that determines the b jet most likely to originate from the top-quark decay. We optimize the neural networks separately for each tagging category and for different lepton categories using different input variables. The variable $M_T^{\ell\nu j}$ is used only for extended muon events, and the output value of the b-jet-selector neural network only for the central-lepton events. In the neural network training, the background samples consist of all backgrounds predicted by simulation, and the fractional yields among background samples are set as predicted by the background model.

TABLE I. Summary of background and signal predictions in two summed tagging categories. The predicted uncertainties include statistical and systematic contributions.

Category	TT+TL	T+LL
$t\bar{t}$	357 ± 40	560 ± 57
Diboson	58.7± 7.8	279 ± 34
Higgs	12.5± 1.0	12.0± 0.9
Z+jets	31.6± 3.5	190 ± 21
Multijet	76 ± 31	326 ± 130
W+heavy-flavor jet	712 ±286	2597 ±1046
W+light-flavor jet	66 ± 14	1220 ± 175
t and tW-channel	53.4± 6.7	265 ± 30
s-channel	116 ± 12	127 ± 12
Total prediction	1484 ±403	5574 ±1501
Observed	1231	5338

We use the pretag sample to check the modeling of each input variable. We investigate the neural-network output in the b-tagged signal region only after ensuring that all variables are well modeled in the control sample. The distributions of neural-network output are shown in Fig. 1, with categories having similar signal purities combined.

We employ a Bayesian binned-likelihood technique to extract the single-top-quark s-channel cross section from the neural-network-output distribution. We assume a uniform prior probability density for all non-negative values of the cross section and integrate the posterior probability density over the prior densities of effects associated with all sources of systematic uncertainties, parametrized using Gaussian priors truncated to avoid negative probabilities. We include the rate uncertainties from the following sources: b-tag scale factor; charm-quark-jet-misidentification rate; light-flavor-jet-misidentification rate; luminosity uncertainties; lepton-acceptance uncertainties; theoretical cross section uncertainties; initial- and final-state radiation; normalization of multijet, Z+jets, and W+jets backgrounds; and jet-energy scale. Shape uncertainties on the final discriminant output that arise from initial-state and final-state radiation, the jet-energy scale, the renormalization and factorization scales, and the electron multijet sample are also taken into account. The standard deviation of the expected cross section distribution obtained from pseudoexperiments is reduced by 17% if the measurement is performed without including any of the systematic uncertainties. The most relevant systematic uncertainties are,

in descending order of importance: the luminosity uncertainties, the b-tag scale-factor uncertainties, the normalization of W+jets, and the uncertainties from initial- and final-state radiation.

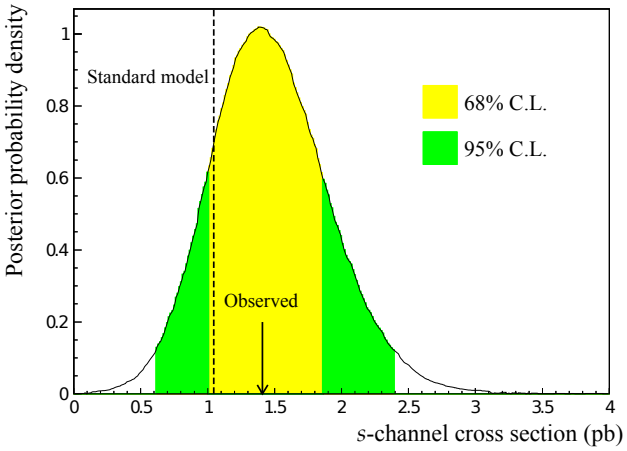

FIG. 2. Posterior probability density distribution for the s-channel cross section measurement, with the SM prediction shown as the vertical dashed line.

The posterior probability density of the s-channel cross section is shown in Fig. 2. The most probable s-channel cross section is $1.41^{+0.44}_{-0.42}$ pb, assuming that the top-quark mass is 172.5 GeV/c^2. This result is in good agreement with the theory prediction calculated at next-to-next-to-leading-order accuracy of 1.05 ± 0.05 pb [25] and the previous measurement from the D0 experiment [10]. The sensitivity is defined to be the significance expected assuming the SM cross section, and as measured from pseudoexperiments with the background-only assumption is 2.9 standard deviations. From background-only pseudoexperiments, we determine the significance of the excess of the measured cross section over the expected backgrounds as corresponding to a p-value of 5.5×10^{-5}, equivalent to 3.8 standard deviations. We interpret the observed excess as evidence of the single-top-quark production through the s-channel process.

In summary, we perform a measurement of the single-top-quark s-channel cross section in the final state with a charged lepton and two jets using the full CDF Run II data set. We find evidence for the single-top-quark s-channel process, and we measure the s-channel cross section to be $1.41^{+0.44}_{-0.42}$ pb, in agreement with the SM prediction.

We thank the Fermilab staff and the technical staffs of the participating institutions for their vital contributions. This work was supported by the U.S. Department of Energy and National Science Foundation; the Italian Istituto Nazionale di Fisica Nucleare; the Ministry of Education, Culture, Sports, Science and Technology of Japan; the Natural Sciences and Engineering Research Council of Canada; the National Science Council of the Republic of China; the Swiss National Science Foundation; the A.P. Sloan Foundation; the Bundesministerium für Bildung und Forschung, Germany; the Korean World Class University Program, the National Research Foundation of Korea; the Science and Technology Facilities Council and the Royal Society, United Kingdom; the Russian Foundation for Basic Research; the Ministerio de Ciencia e Innovación, and Programa Consolider-Ingenio 2010, Spain; the Slovak R&D Agency; the Academy of Finland; the Australian Research Council (ARC); and the EU community Marie Curie Fellowship Contract No. 302103.

* Deceased
† With visitors from [a]University of British Columbia, Vancouver, BC V6T 1Z1, Canada, [b]Istituto Nazionale di Fisica Nucleare, Sezione di Cagliari, 09042 Monserrato (Cagliari), Italy, [c]University of California Irvine, Irvine, CA 92697, USA, [d]Institute of Physics, Academy of Sciences of the Czech Republic, 182 21, Czech Republic, [e]CERN, CH-1211 Geneva, Switzerland, [f]Cornell University, Ithaca, NY 14853, USA, [g]University of Cyprus, Nicosia CY-1678, Cyprus, [h]Office of Science, U.S. Department of Energy, Washington, DC 20585, USA, [i]University College Dublin, Dublin 4, Ireland, [j]ETH, 8092 Zürich, Switzerland, [k]University of Fukui, Fukui City, Fukui Prefecture, Japan 910-0017, [l]Universidad Iberoamericana, Lomas de Santa Fe, México, C.P. 01219, Distrito Federal, [m]University of Iowa, Iowa City, IA 52242, USA, [n]Kinki University, Higashi-Osaka City, Japan 577-8502, [o]Kansas State University, Manhattan, KS 66506, USA, [p]Brookhaven National Laboratory, Upton, NY 11973, USA, [q]Queen Mary, University of London, London, E1 4NS, United Kingdom, [r]University of Melbourne, Victoria 3010, Australia, [s]Muons, Inc., Batavia, IL 60510, USA, [t]Nagasaki Institute of Applied Science, Nagasaki 851-0193, Japan, [u]National Research Nuclear University, Moscow 115409, Russia, [v]Northwestern University, Evanston, IL 60208, USA, [w]University of Notre Dame, Notre Dame, IN 46556, USA, [x]Universidad de Oviedo, E-33007 Oviedo, Spain, [y]CNRS-IN2P3, Paris, F-75205 France, [z]Universidad Tecnica Federico Santa Maria, 110v Valparaiso, Chile, [aa]The University of Jordan, Amman 11942, Jordan, [bb]Universite catholique de Louvain, 1348 Louvain-La-Neuve, Belgium, [cc]University of Zürich, 8006 Zürich, Switzerland, [dd]Massachusetts General Hospital, Boston, MA 02114 USA, [ee]Harvard Medical School, Boston, MA 02114 USA, [ff]Hampton University, Hampton, VA 23668, USA, [gg]Los Alamos National Laboratory, Los Alamos, NM 87544, USA, [hh]Università degli Studi di Napoli Federico I, I-80138 Napoli, Italy

[1] T. M. P. Tait and C.-P. Yuan, Phys. Rev. D **63**, 014018 (2000).
[2] The third process, tW production, contributes negligibly in $p\bar{p}$ collisions, given the cross section of 0.25 pb [25] .

[3] T. Aaltonen *et al.* (CDF Collaboration), Phys. Rev. Lett. **103**, 092002 (2009).

[4] V. M. Abazov *et al.* (D0 Collaboration), Phys. Rev. Lett. **103**, 092001 (2009).

[5] V. Abazov *et al.* (D0 Collaboration), Phys. Lett. B **705**, 313 (2011).

[6] G. Aad *et al.* (ATLAS Collaboration), Phys. Lett. B **717**, 330 (2012).

[7] S. Chatrchyan et al. (CMS Collaboration), J. High Energy Phys. 12 (2012) 035.

[8] G. Aad *et al.* (ATLAS Collaboration), Phys. Lett. B **716**, 142 (2012).

[9] S. Chatrchyan *et al.* (CMS Collaboration), Phys. Rev. Lett. **110**, 022003 (2013).

[10] V. Abazov *et al.* (D0 Collaboration), Phys. Lett. B **726**, 656 (2013).

[11] D. Acosta *et al.* (CDF Collaboration), Phys. Rev. D **71**, 032001 (2005).

[12] T. Aaltonen *et al.* (CDF Collaboration), Phys. Rev. Lett. **109**, 111804 (2012).

[13] T. Aaltonen *et al.* (CDF Collaboration), Phys. Rev. D **82**, 112005 (2010).

[14] J. Freeman, T. Junk, M. Kirby, Y. Oksuzian, T. Phillips, F. Snider, M. Trovato, J. Vizan, and W. Yao, Nucl. Instrum. Methods Phys. Res., Sect. A **697**, 64 (2013).

[15] We use a cylindrical coordinate system with the origin at the center of the CDF II detector, z pointing in the direction of the proton beam, θ and ϕ representing the polar and azimuthal angles, respectively. The transverse energy E_T is defined to be $E\sin\theta$. The calorimeter missing E_T ($\vec{\not\!\!E}_T$(cal)) is defined by the sum over calorimeter towers $\vec{\not\!\!E}_T(\text{cal}) = -\sum_i E_T^i \hat{n}_i$, where i is an index over calorimeter tower with $|\eta| < 3.6$, and $\hat{n}_i$ is a unit vector perpendicular to the beam axis and pointing at the ith calorimeter tower. The reconstructed missing energy, $\vec{\not\!\!E}_T$, is derived by correcting $\vec{\not\!\!E}_T$(cal) for muon energy deposition and jet-energy adjustments. We define $\not\!\!E_T$(cal) and $\not\!\!E_T$ to be the scalar magnitudes of $\vec{\not\!\!E}_T$(cal) and $\vec{\not\!\!E}_T$, respectively.

[16] F. Sforza, V. Lippi, and G. Chiarelli, J. Phys. Conf. Ser. **331**, 032045 (2011).

[17] R. Brun, F. Carminati, and S. Giani, *GEANT Detector Description and Simulation Tool*, Tech. Rep. CERN-W5013 (1994).

[18] S. Alioli, P. Nason, C. Oleari, and E. Re, J. High Energy Phys. 09 (2009) 111.

[19] T. Sjöstrand, S. Mrenna, and P. Skands, J. High Energy Phys. 05 (2006) 026.

[20] J. M. Campbell and R. K. Ellis, Phys. Rev. D **60**, 113006 (1999).

[21] M. Cacciari, S. Frixione, G. Ridolfi, M. L. Mangano, and P. Nason, J. High Energy Phys. 04 (2004) 068.

[22] J. Baglio and A. Djouadi, J. High Energy Phys. 10 (2010) 064.

[23] M. L. Mangano, F. Piccinini, A. D. Polosa, M. Moretti, and R. Pittau, J. High Energy Phys. 07 (2003) 001.

[24] A. Hoecker *et al.*, PoS **ACAT**, 040 (2007).

[25] N. Kidonakis, Phys. Rev. D **81**, 054028 (2010).